



# Enhanced Photocatalytic Activity of Conducting Polypyrrole-TiO<sub>2</sub> Nanocomposite for Degradation of Organic Dyes under UV Light Irradiation

M. Sangareswari, M. Meenakshi Sundaram\*

Centre for Research and Post Graduate Studies in Chemistry, Ayya Nadar Janaki Ammal College, Sivakasi – 626 124, TN, India.

## ARTICLE DETAILS

### Article history:

Received 13 August 2015

Accepted 22 August 2015

Available online 07 September 2015

### Keywords:

Nanocomposite  
Methylene Blue  
Acid Orange 7  
Photodegradation  
UV Light

## ABSTRACT

The objective of this study was to investigate and compare the kinetic and photocatalytic activity of conducting polypyrrole-TiO<sub>2</sub> nanocomposite for the degradation of Methylene Blue (MB) and Acid Orange 7 (A07) dyes under UV light irradiation. Conducting polypyrrole-TiO<sub>2</sub> nanocomposite was synthesised by chemical oxidative polymerization method. The synthesised nanocomposite was characterized by TEM, SEM-EDAX, XRD, FT-IR and UV-DRS analysis. The effect of TiO<sub>2</sub> nanoparticles embedded into conducting polypyrrole on the morphology, structure and crystalline size of the conducting polypyrrole is studied by these techniques. A possible photocatalytic mechanism for the degradation of organic dyes was also investigated. The effect of various operational parameters like concentration, time, catalyst loading and pH on dyes were studied. This result indicates that conducting polypyrrole-TiO<sub>2</sub> nanocomposite shows high photocatalytic performance for the degradation of methylene blue and acid orange 7 dyes under UV system.

## 1. Introduction

Large amount of dye are annually produced and applied in different industries including textile, cosmetic, paper, leather, pharmaceutical and nutrition industries. Dyes are an important class of aquatic pollutants and are becoming a major source of environmental contamination [1-2]. Different techniques such as adsorption, oxidation, reduction, electrochemical and membrane filtration are applied to remove these pollutants from the industrial effluents. Among these methods photodegradation is one of the easiest method to remove the dye from the water environment [3].

Photocatalysis has been considered most as one of the most promising technologies because it represents an economical and green way to degrade pollutants by utilizing the energy of either natural sunlight or artificial indoor illumination, which is abundantly available everywhere in the world. In the photo-decomposition or photo-oxidation of hazardous substances, photocatalyst holds great potentials for the acceleration of photoreactions [4-7].

Heterogeneous photocatalysis with TiO<sub>2</sub> as a semiconductor has proven to be an efficient process for elimination of a large number of dyes from textile wastewater.

The main disadvantage to its effective utilization are obvious. The concentration of photo-generated electron-hole pairs is reduced by the inherent recombination process leading to the destruction of active electron-hole pairs and further resulting in low photocatalytic activity. Conjugated polymers with extend bi-conjugated electron systems such as polythiophene and polypyrrole have shown great promise, due to their high absorption coefficients in the visible part of the spectrum, high mobility of charge carriers, good environmental stability [8-10].

Recently, a little work has been done on using conjugated polymers – modified TiO<sub>2</sub> to degrade organic pollutant since nanocomposites of conductive polymers and inorganic particles show interesting physical properties and application potential.

In this paper, we have prepared TiO<sub>2</sub> nanoparticles modified by a small amount of PPy. The modified conducting polypyrrole-TiO<sub>2</sub> nanocomposite further investigated by the degradation of acid orange and methylene blue dyes.

## 2. Experimental Methods

### 2.1 Materials

The semiconductor TiO<sub>2</sub> nanoparticles with particle size of ~21nm purchased from Sigma-Aldrich Chemicals. The oxidant ammonium persulfate (APS) was received from Thomas Baker Chemicals. Pyrrole (98+%) obtained from Alfa Aesar company. The commercial organic dyes methylene blue (molecular formula= C<sub>16</sub>H<sub>18</sub>N<sub>3</sub>SCl; λ<sub>max</sub> = 665 nm) (Fig. 1a) and acid orange 7 (molecular formula= C<sub>16</sub>H<sub>11</sub>N<sub>2</sub>NaO<sub>4</sub>S; λ<sub>max</sub> = 490 nm) (Fig. 1b) were purchased from Qualigens Fine Chemicals. Double distilled water was used throughout this study for the preparation of all the experimental solutions.

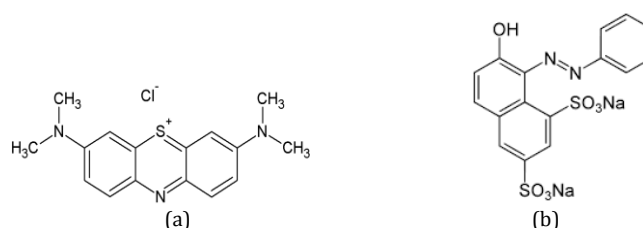


Fig. 1 a) Structure of MB dye; b) Structure of A07 dye

### 2.2 Synthesis of Conducting Polypyrrole -TiO<sub>2</sub> Nanocomposites

Pyrrole (5 mmol) was dissolved in 0.1 M sulphuric acid solution. The TiO<sub>2</sub> nanoparticles were added to the above prepared solution. The solution was oxidized using ammonium persulfate solution was added drop by drop with constant stirring under 50 °C cooled condition. After continuous stirring, the solution becomes precipitated at brown coloured. The obtained product was washed with distilled water to remove the residual ammonia solution. Finally the product was dried at room temperature at overnight.

### 2.3 Instrumental Analysis

UV-visible spectrum (DRS) was recorded using UV-Visible spectrophotometer ("SHIMADZU" model: UV 2450). FT-IR spectra of the purified samples were measured using FT-IR spectrophotometer ("SHIMADZU" (Model: 8400S) spectrometer). The crystallographic

\*Corresponding Author

Email Address: [drmsundaram61@gmail.com](mailto:drmsundaram61@gmail.com) (M. Meenakshi Sundaram)

structures of the materials were determined by high resolution powder diffractometer (Model–RICH SIEFRT&CO with Cu as the X - ray source ( $\lambda = 1.5406 \times 10^{-10}$  m). The surface morphology of the sample was recorded using Scanning Electron Microscopy and Energy Dispersive X-ray Analysis (SEM-EDAX) (Model: FEG Quantum 250 EDAX). TEM analysis was done by High Resolution Transmission Electron Microscopy (HRTEM) and Small Area Electron Diffraction (SAED) using FEI Tecnai F20 Transmission Electron microscope.

#### 2.4 Photocatalytic Activity

The prepared dye solutions methylene blue and acid orange 7 both are taken in UV multilamp photoreactor tube. The required amount (0.020 g) of synthesised material was added to the above dye solution. Before irradiation the dye solutions were kept under dark condition for 30 min to obtain adsorption-desorption equilibrium. Then it kept inside UV multilamp photoreactor for 75 min. The collected suspension was centrifuged and filtered before the UV-visible absorption measurements. The degradation rate of both dyes were estimated by the following equation,

$$\text{Percentage removal (\% R)} = \left[ \frac{C_i - C_f}{C_i} \right] \times 100 \quad (1)$$

where,  $C_i$  &  $C_f$  is the initial & final concentration of dye (ppm) at a given time

### 3. Results and Discussion

#### 3.1 Transmission Electron Microscopy (TEM) Analysis

The TEM picture of conducting polypyrrole-TiO<sub>2</sub> nanocomposite Fig. 2a shows that the particles have mixed shapes. The TEM micrographs reveal a wide distribution of hexagonal and spherical particles. The TEM micrograph of conducting polypyrrole-TiO<sub>2</sub> nanocomposite Fig. 2b shows that TiO<sub>2</sub> nanoparticles are homogeneously dispersed in the polypyrrole matrix [11,12].

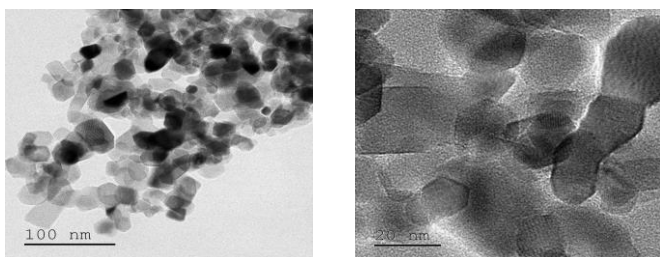


Fig. 2 TEM images for conducting polypyrrole-TiO<sub>2</sub> nanocomposite

#### 3.2 Scanning Electron Microscopy (SEM) Analysis

The surface morphology of the synthesised conducting polypyrrole-TiO<sub>2</sub> nanocomposite was investigated by using scanning electron microscopy (SEM). The synthesised polypyrrole having flower like structure which are shown in Fig. 3a. The TiO<sub>2</sub> nanoparticles are ball like spherical shape they are well deposited on the surface polypyrrole as illustrated in Fig. 3b [13,14].

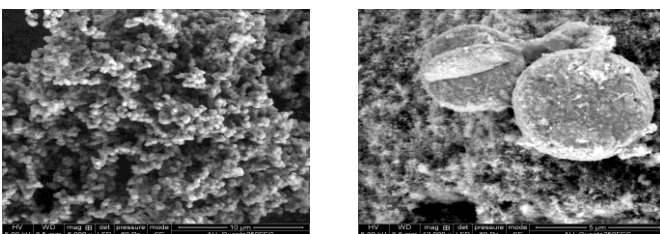


Fig. 3 SEM images for Conducting Polypyrrole-TiO<sub>2</sub> nanocomposite

#### 3.3 X-ray Diffraction (XRD) Analysis

The crystallographic structure of obtained conducting polypyrrole - TiO<sub>2</sub> nanocomposite was evidenced by XRD measurements. Fig. 4 shows the XRD pattern of conducting polypyrrole-TiO<sub>2</sub> nanocomposite. The XRD peaks denote the formation of conducting polypyrrole-TiO<sub>2</sub> nanocomposite in crystalline size. The respected peaks occur at 25.3°, 26.2°, 36.0°, 38.2°, 48.9°, 54.3°, 56.6°, 63.1° and 69.9°. Moreover, it can be noted that due to the TiO<sub>2</sub> was deposited on the surface of polypyrrole. The

mean crystalline sizes of conducting polypyrrole-TiO<sub>2</sub> nanocomposite calculated by using Scherrer's formula.

$$D \text{ scherrer} = k\lambda/\beta \cos \Theta \quad (2)$$

Where,  $\lambda$  is the wavelength of the X-ray radiation ( $\lambda = 1.54 \times 10^{-9}$ nm),  $k$  is the Scherrer constant ( $k = 0.89$ ),  $\Theta$  is the diffraction angle and  $\beta$  is the line width at half-maximum height of the most intense peak. Based on the XRD results, the crystalline size of conducting polypyrrole-TiO<sub>2</sub> nanocomposites is 8.3 nm. The results are in good agreement with the TEM images.

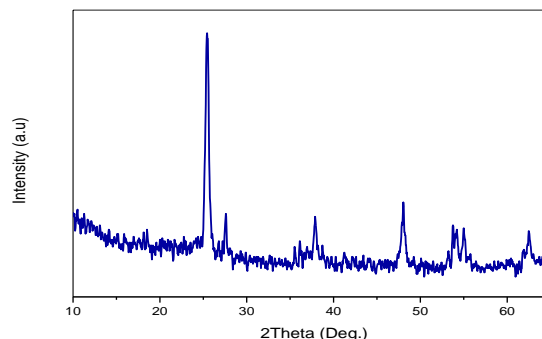


Fig. 4 XRD for conducting polypyrrole-TiO<sub>2</sub> nanocomposite

#### 3.4 UV-DRS Analysis

The optical properties of PPy-TiO<sub>2</sub> nanocomposites investigated by UV-DRS spectroscopy as shown in Fig. 5A. From the UV-DRS analysis we can measure band gap of the synthesised conducting polypyrrole-TiO<sub>2</sub> nanocomposite. The position of fundamental absorption edge of conducting polypyrrole-TiO<sub>2</sub> nanocomposite is determined using equation,

$$(\alpha h\nu)^2 = A (h\nu - E_g)^n \quad (3)$$

Where  $\alpha$ ,  $h$ ,  $\nu$ ,  $E_g$  and  $A$  are the absorption coefficients, Plank constant, light frequency, band gap and a constant, respectively. The  $n$  value depends on the transition characteristics. The  $E_g$  value can be estimated by extrapolating the straight portion of the  $(\alpha h\nu)^2 - (h\nu)$  plot which is shown in Fig. 5B. The band gap for the prepared conducting polypyrrole-TiO<sub>2</sub> nanocomposite show lower band gap value as 2.1 eV than compared to the other components like TiO<sub>2</sub> (3.2 eV) and PPy (2.4 eV).

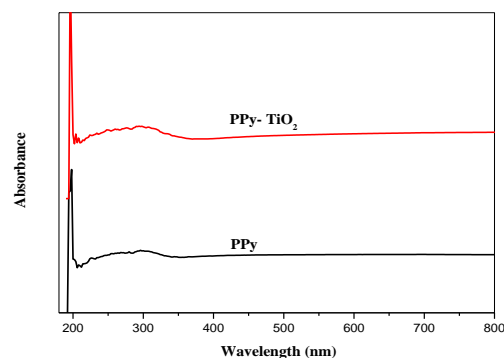


Fig. 5A UV-DRS for polypyrrole and conducting polypyrrole-TiO<sub>2</sub> nanocomposite

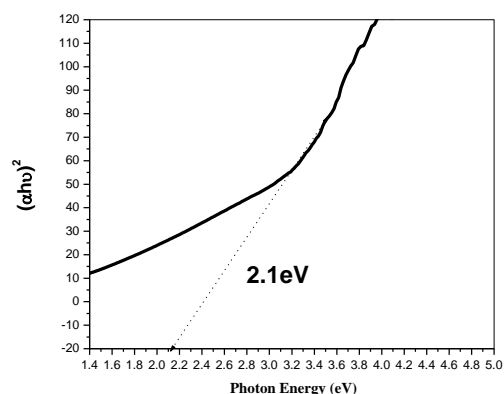


Fig. 5B Band gap for conducting polypyrrole-TiO<sub>2</sub> nanocomposite

### 3.5 FT-IR Analysis

Fig. 6 shows the typical FTIR spectra of PPy polymer, the bands at 1552.15 and 1635.13 $\text{cm}^{-1}$  are ascribed to the stretching vibrations of C=C and C=N in the phenazine ring, respectively. The peaks at 1400.22 and 1100  $\text{cm}^{-1}$  are ascribed with the C-N stretching in the benzenoid and quinoid imine units. Moreover, the bands at 520.78  $\text{cm}^{-1}$  denoted the C-H out-of plane bending vibrations of benzene nuclei of PPy. The TiO<sub>2</sub> showed a broad band below 638 $\text{cm}^{-1}$ , which is attributed to the Ti–O–Ti stretching and bending vibrational modes [15–18].

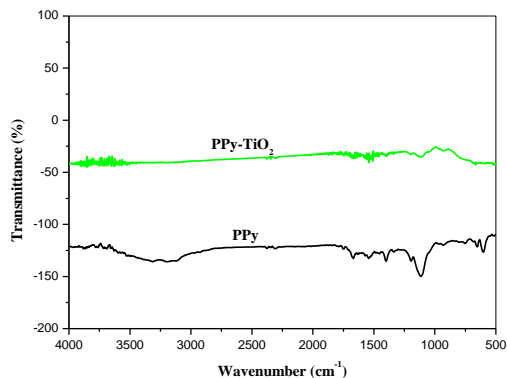


Fig. 6 FT-IR for polypyrrole and conducting polypyrrole-TiO<sub>2</sub> nanocomposite

### 3.6 Photo Degradation Studies

#### 3.6.1 Effect of Concentration of Dyes

The photocatalytic decoloration of methylene blue and acid orange 7 was carried out at different initial concentrations ranging from 10 ppm to 50 ppm under UV light systems. The effect of concentration of dye molecules increases the percentage removal was decreases. Because more number of dye molecules are adsorbed on the surface of the photocatalyst. So the photon entering pathway will be reduced. The degradation of methylene blue and acid orange dyes as shown in Fig. 7 [19–20].

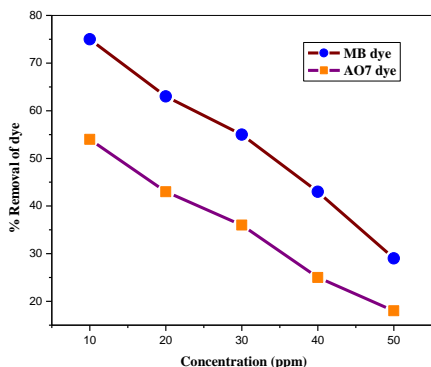


Fig. 7 Effect of concentration of MB and AO7 dye

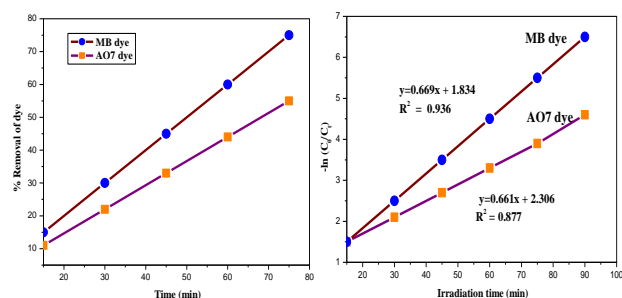


Fig. 8 Time variation for MB and AO

Fig. 9 Kinetics for MB and AO dye

#### 3.6.2 Effect of Time Variation

Fig. 8 reveals the effect of time variation for both MB and AO7 dyes. When time increases the percentage removal of dye also increases. The results of experiments showed that the photocatalytic degradation of MB dye and AO 7 dye obey apparently pseudo first order kinetics and the rate expression is given by the following equation,

$$\ln(C_0/C_t) = kt \quad (4)$$

Where, Co = initial concentration of dye solution

Ct = final concentration of dye solution in various time interval

k = is the pseudo-first order rate constant for degradation of dye  
t = is the irradiation time respectively.

The value of  $\ln(C_0/C_t)$  is plotted against time and the plots are found to be linear as shown in Fig. 9.

#### 3.6.3 Effect of Dose Variation

The amount of catalyst increases from 12 mg to 20 mg. The increase in the efficiency seems to be due to the increase in the total surface area, namely number of active sites available for the photo catalytic reaction as the dosage of photo catalyst increased as illustrated as Fig. 10. However, when photocatalyst was overdosed, the number of active sites on the photocatalyst surface may become almost constant because of the decreased light penetration, the increased light scattering and the loss in surface area occasioned by agglomeration at high solid concentration [21–26].

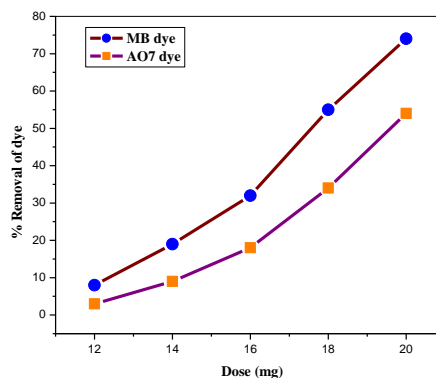


Fig. 10 Dose variation for MB and AO7 dye

#### 3.6.4 Effect of pH Variation

The wastewater from textile industries usually has a wide range of pH values. Further, the generation of hydroxyl radicals is also a function of pH. The pH values increases from 3 to 11 for both dyes. The zero point charge for TiO<sub>2</sub> is 6.25. In acid orange 7 dye the pH values 3, 5 and 7 higher percentage (76%, 73% and 70%) removal was occur because at this acidic condition the surface of the catalyst will become positively charged so the anionic dye (acid orange 7) easily attracted by the catalyst. So higher percentage removal occur in acidic condition. In contrast, methylene blue dye pH increases from 3 to 11 higher percentage removal (at basic condition) was occurred. In this condition the surface of the catalyst will become negatively charged. So methylene blue dye easily attracted by the catalyst. The above said procedure is shown in Fig. 11 [27–29].

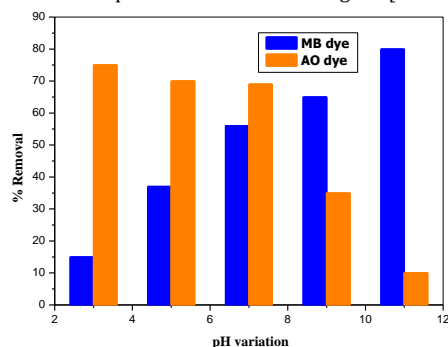


Fig. 11 Effect of pH variation for MB and AO7 dye

#### 3.6.5 Mechanism

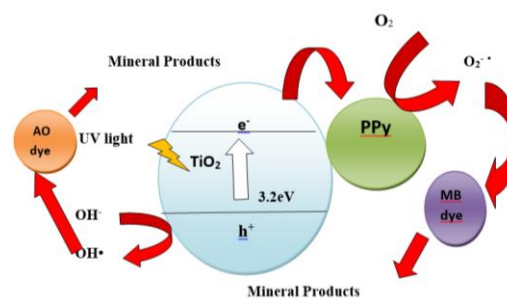


Fig. 12 Possible pathway of the photoelectron transfer excited by UV light irradiation including the photocatalytic process for modified TiO<sub>2</sub> nanoparticles

### 3.6.6 Stability of Catalyst

The reproducibility of the photocatalytic degradation activity of a 0.02 g sample conducting polypyrrole-TiO<sub>2</sub> nanocomposite performed on a 10 ppm MB solution (50 mL) is expressed as the number of cycles. Where the photocatalytic degradation of the nanocomposite was reduced from 75% on the first usage to 65%, 60% and 40% after the second, third and fourth cycles of reuse, respectively. This reduced dye photodegradation activity is in accord with the appearance of recycled conducting polypyrrole-TiO<sub>2</sub> nanocomposite, which was clearly changed in the morphology of the PPy-TiO<sub>2</sub> nanocomposites due to the Photodegradation.

### 4. Conclusion

The conducting polypyrrole-TiO<sub>2</sub> nanocomposite was successfully prepared by chemical oxidative polymerization method. The results from TEM and SEM analysis consistently indicate that the TiO<sub>2</sub> nanoparticles was deposited on polypyrrole matrix. The FT-IR results show the main functional group present in conducting polypyrrole -TiO<sub>2</sub> nanocomposites. The UV-Vis diffuse reflectance spectra confirmed that the modified catalyst absorbed more photons under light irradiation. The organic dyes were successfully degraded by the prepared nanocomposite under light UV irradiation. The synthesised nanocomposite could be used for removal of waste water which contributes to the environmental pollution.

### Acknowledgement

The authors thank UGC, Delhi for providing financial support and The Management, Ayya Nadar Janaki Ammal College, Sivakasi for providing lab facilities to carry out this research work.

### References

- [1] A. Mills, S. Lunte, An overview of semiconductor photocatalysis, *J. Photochem. Photobiol. A* 108 (1997) 1–35.
- [2] S. Hager, R. Bauer, Heterogeneous photocatalytic degradation of organics by uv-irradiated titanium dioxide for air purification, *Chemosphere* 38 (1999) 1549–1559.
- [3] M.R. Hoffman, S.T. Martin, W. Choi, D.W. Bahnemann, Environmental applications of semiconductor photocatalysis, *Chem. Rev.* 95 (1995) 69–95.
- [4] P. Muthirulan, C. Nirmala Devi, M. Meenakshi Sundaram, Synchronous role of coupled adsorption and photocatalytic degradation on CAC-TiO<sub>2</sub> composite generating excellent mineralization of alizarin cyanine green dye in aqueous solution, *Arab. J. Chem.* 1 (2012) 1–7.
- [5] P. Muthirulan, C. Kannan, Nirmala Devi, M. Meenakshi Sundaram, Facile synthesis of novel hierarchical TiO<sub>2</sub>@Poly(o-phenylenediamine) core-shell structures with enhanced photocatalytic performance under solar light, *J. Environ. Chem. Eng.* 1 (2013) 620–627.
- [6] A.R. Khataee, M.B. Kasiri, Photocatalytic degradation of organic dyes in the presence of nanostructured titanium dioxide: Influence of the chemical structure of dyes, *J. Mol. Catal. A: Chem.* 328 (2010) 8–26.
- [7] B.N. Narayanan, Photodegradation of methyorange over zirconia doped TiO<sub>2</sub> using solar energy, *Europ. J. Sci. Res.* 4 (2009) 566–571.
- [8] D. Wang, J. Zhang, Q. Luo, X. Li, Y. Duan, J. An, Characterization and photocatalytic activity of poly(3-hexylthiophene)-modified TiO<sub>2</sub> for degradation of methyl orange dye under visible light, *J. Hazard. Mater.* 169 (2009) 546–550.
- [9] G. Zayani, L. Bousseelmi, F. Mhenni, A. Ghrabi, Solar photocatalytic degradation of commercial textile azo dyes: Performance of pilot plant scale thin film fixed-bed photoreactor, *Desalin.* 248 (2009) 23–31.
- [10] M.A. Salem, A.F. Ghonemiy, A.B. Zaki, Photocatalytic degradation of Allura red and Quinoline yellow with polyaniline/ TiO<sub>2</sub> nanocomposite, *Appl. Catal. B: Environ.* 91 (2009) 59–66.
- [11] M. Hosokawa, K. Nogi, M. Naito, T. Yokoyama, *Nanoparticle Technology Handbook*, Elsevier, Amsterdam, 2007.
- [12] M.R. Mahmoudian, Y. Alias, W.J. Basirun, M. Ebadi, Effects of different polypyrrole/TiO<sub>2</sub> nanocomposite morphologies in polyvinyl butyral coatings for preventing the corrosion of mild steel, *Appl. Surf. Sci.* 268 (2013) 302–311.
- [13] M. Sangareswari, M. Meenakshi Sundaram, A comparative study on photocatalytic efficiency of TiO<sub>2</sub> and BiVO<sub>4</sub> nanomaterial for degradation of methylene blue dye under sunlight irradiation, *J. Adv. Chem. Sci.* 1(2) (2015) 75–77.
- [14] M. Meenakshi Sundaram, M. Sangareswari, P. Muthirulan, Enhanced photocatalytic activity of polypyrrole/TiO<sub>2</sub> nanocomposites for acid violet dye degradation under UV irradiation, *Int. J. Innov. Res. Sci. Eng.* 2 (2014) 420–423.
- [15] F. Denga, Y. Li, X. Luob, Y. Lixia,, X. Tu, Preparation of conductive polypyrrole/TiO<sub>2</sub> nanocomposite via surface molecular imprinting technique and its photocatalytic activity under simulated solar light irradiation, *Colloid Surf A: Physicochem. Eng. Aspects.* 395 (2012) 183–189.
- [16] S. Deivanayaki, V. Ponnuswamy, P. Jayamurugan, S. Ashokan, The structure and properties of polypyrrole/titaniumdioxide nanospheres of various dopant percentages by chemical oxidation method, *Elixir polymer* 49B (2012) 10182–10185
- [17] E.T. Kang, K.G. Noho, K.L. Tan, polyaniline: a polymer with many interesting intrinsic redox states, *Journal of progress in polymer science*, 23 (1998) 277–324.
- [18] X. You-nan, J.M. Wiesinger, A.G. Macdiarmid, A.J. Epstein, Camphorsulfonic acid fully doped polyaniline emeraldine salt: Conformations in different solvents studied by an ultraviolet/visible/near-infrared spectroscopic method, *J. Chem. Mater.* 7(3) (1995) 443–445.
- [19] L.G. Devi, S.G. Kumar, Influence of physicochemical-electronic properties of transition metal ion doped polycrystalline titania on the photocatalytic degradation of Indigo Carmine and 4- nitrophenol under UV/solar light. *Appl. Surf. Sci.* 257 (2011) 2779–2790.
- [20] M.R. Hoffmann, S.T. Martin, W. Choi, D.W. Bahnemann, Environmental applications of semiconductor photocatalysis, *Chem. Rev.* 95 (1995) 69–96.
- [21] A. Fujishima, K. Honda, Electrochemical photolysis of water at a semiconductor electrode, *Nature* 238 (1972) 37–38.
- [22] A. Kudo, Y. Miseki, Heterogeneous photocatalyst materials for water splitting. *Chem. Soc. Rev.* 38 (2009) 253–278.
- [23] Y.H. Tseng, C.H. Kuo, Photocatalytic degradation of dye and NO<sub>x</sub> using visible-light-responsive carboncontaining TiO<sub>2</sub>, *Catal. Today.* 174 (2011) 114–120.
- [24] A.A. Ismaila, R.A. Geiushya, H. Bouzid, S.A. AlSayari, A. Al-Hajry, D.W. Bahnemann, TiO<sub>2</sub> decoration of graphene layers for highly efficient photocatalyst: impact of calcination at different gas atmosphere on photocatalytic efficiency, *Appl. Catal. B: Environ.* 29 (2013) 129–132.
- [25] V.K. Gupta, R. Jain, A. Mittal, T.A. Saleh, A. Nayak, S. Agarwal, S. Sikarwar, Photocatalytic degradation of toxic dye amaranth on TiO<sub>2</sub>/UV in aqueous suspensions, *Mater. Sci. Eng.* 32 (2012) 12–17.
- [26] S.A. Abo-Farha, Photocatalytic degradation of monoazo and diazo dyes in wastewater on nanometer-sized TiO<sub>2</sub>, *Researcher* 2 (2010) 1–20.
- [27] D.S. Ibrahim, A.P. Anand, A. Muthukrishnaraj, R. Thilakavathi, N. Balasubramanian, In situ electrocatalytic treatment of a reactive golden yellow HER synthetic dye effluent, *J. Environ. Chem. Eng.* 5 (2013) 2–8.
- [28] S. Chatterjee, S.R. Lim, S.H. Woo, Removal of reactive black 5 by zero-valent iron modified with various surfactants, *Chemical Eng. J.* 160 (2010) 27–32.
- [29] R. Yuvakkumar, V. Elango, V. Rajendran, N. Kannan, Preparation and characterization of zerovalent iron nanoparticles, *Digest J. Nanomaterials Biostructures*, 6 (2011) 1771–1776.